Applied Physics Letters

Thermal conductivity of $SrTiO_3$ under high-pressure

Cite as: Appl. Phys. Lett. **120**, 262201 (2022); https://doi.org/10.1063/5.0098353
Submitted: 08 May 2022 • Accepted: 10 June 2022 • Published Online: 27 June 2022

Zhongyin Zhang, Kunpeng Yuan, Jie Zhu, et al.

Applied Physics Letters ARTICLE scitation.org/journal/apl

Thermal conductivity of $SrTiO_3$ under high-pressure

Cite as: Appl. Phys. Lett. **120**, 262201 (2022); doi: 10.1063/5.0098353
Submitted: 8 May 2022 · Accepted: 10 June 2022 ·
Published Online: 27 June 2022

Zhongyin Zhang, Kunpeng Yuan, Jie Zhu,[a] Xuanhui Fan, Jing Zhou, and Dawei Tang[a]

AFFILIATIONS

Key Laboratory of Ocean Energy Utilization and Energy Conservation of Ministry of Education, Dalian University of Technology, Dalian 116023, Liaoning, People's Republic of China

[a]Authors to whom correspondence should be addressed: zhujie@dlut.edu.cn and dwtang@dlut.edu.cn

ABSTRACT

Pressure is an effective way to regulate physical properties of ABO_3 perovskites, such as thermal conductivity κ of $SrTiO_3$, which can enhance fundamental understanding of structure–property relationships. In this Letter, κ of $SrTiO_3$ was investigated up to ~20 GPa using high-pressure time domain thermoreflectance together with Raman spectroscopy and first-principles calculations. Our theoretical predictions effectively explain the measured results. In both cubic and tetragonal phases, κ increased with compression, and optical phonons are the dominant heat carriers. The phonon group velocity and relaxation time make prominent contributions to κ with compression in the cubic phase, while the reduction in the anharmonicity of phonon modes and the phonon scattering channels dominates the increase in κ in the tetragonal phase. Especially, during the transition from cubic to tetragonal phases, there is a significant drop in κ, which originally results from the TiO_6 octahedral distortion induced by the soft-phonon-mode, which markedly reduces the phonon group velocity. Our results not only help reveal the pressure effect on κ of complex oxides but also pave their way for applications on high-temperature superconductors and spin devices.

钙钛矿

Perovskites are particularly interesting materials since even slight regulations, such as isotope substitution,[1] chemical doping,[2] and external pressure,[3] can generate obvious changes in physical and chemical properties. Strontium titanate ($SrTiO_3$), as model ABO_3 perovskites, exhibits a variety of phase transitions as a result of a delicate balance between fluctuation effects[4] and a quantum-mechanical driving force,[5] which lead to symmetry reduction. For instance, pressure will reduce zone-center ferroelectricity but increase anti-ferrodistortive tilt instabilities at the zone-boundary.[6] Hence, the complex behaviors accompanied by structural transitions are of fundamental importance and have attracted widespread interest in applications in superconductors,[7] microelectronics,[8] and spin devices.[9]

Applying external pressure on $SrTiO_3$ can advance our fundamental understanding of structure–property relationships. Previous studies on $SrTiO_3$ at high-pressure mainly focused on pressure-induced structural transitions. Many optical techniques, such as Brillouin,[10] Raman spectroscopy,[11,12] x-ray diffraction,[11] and inelastic x-ray scattering,[13] have been employed to prove that $SrTiO_3$ undergoes anti-ferrodistortive phase transitions at 6–9 GPa, where the structure changes from a cubic to tetragonal phase. The change in interatomic forces under high-pressure favors the lower-symmetry tetragonal phase.[13] Similar to the impact of low temperatures,[14] the pressure-induced phase transition mechanism is attributed to the soft-phonon-mode, which leads to the elongation and tilt of the TiO_6 octahedral in the tetragonal phase.[15] While the tilt reduces the volume of the unit cell, the elongation increases it. The balance between the two effects is complex and not simply proportional to the tilt angle itself. Aside from that, Zhang *et al.*[16] have investigated size-dependent cubic to tetragonal transitions on $SrTiO_3$ nanoparticles, finding that the transition pressure decreases with decreasing particle size. The structural transitions of $SrTiO_3$ under high-pressure have been thoroughly studied, while several reports have also devoted to comprehend the elasticity[17] and optical and electronic properties[18] of $SrTiO_3$. However, because of the significant challenge in the experimental technique, the observation of $SrTiO_3$ phonon transport behaviors under high-pressure is thus far lacks. The role of the soft-phonon-mode on thermal conductivity κ in $SrTiO_3$ remains elusive under high-pressure despite the fact that assessing the contribution of the particular phonon mode on κ is of great interest.

In this work, time domain thermoreflectance (TDTR) integrated with a diamond anvil cell (DAC), a powerful method for measuring optical[19] and thermal[20,21] properties under high-pressure, was employed

to characterize κ of $SrTiO_3$ up to ~20 GPa. High-pressure Raman spectroscopy was also implemented to investigate structure transitions. Combined with first-principles calculations, the underlying mechanism of pressure regulation on κ of $SrTiO_3$, especially the κ changing with cubic to tetragonal phase transitions, was first unveiled at the phonon mode level.

In our experiment, two identical $SrTiO_3$ samples were prepared for either structure characterization by high-pressure Raman spectroscopy or thermal measurements through high-pressure TDTR with a DAC (Fig. 1). The one for TDTR measurement had been coated with a ~90 aluminum (Al) film before loading into the DAC. The sample encapsulation procedures, TDTR experiment details, and Raman spectroscopy were described in detail in the supplementary material. In addition, the ruby spectra at the selected pressure were also presented in Fig. S1 of the supplementary material. Raman spectroscopy was employed to track structural transitions in $SrTiO_3$ up to ~17 GPa, shown in Fig. 2(a). In the cubic phase of $SrTiO_3$, first-order Raman scattering is forbidden by symmetry;[11] however, a strong and broad scattering signature is observed. These broad bands are associated with the second-order Raman spectra and their intensity decreases significantly with compression. For convenience, we assign peak positions using letters A, B, and C in an alphabetical order from low to high frequencies. The two first-order peaks with $E_g + B_{1g}$ symmetry emerge at 6.6 GPa, revealing the structural transition (anti-ferrodistortive) to the tetragonal phase, which is in agreement with earlier reports.[16,22,23] The soft mode of A_{1g} symmetry is followed down to 79 cm^{-1} at ~12.3 GPa, which is fitted by an expression of the form $\omega^2 = a \times (P - P_c)$, giving a critical pressure of $P_c = 6.6$ GPa.

The evolution of the Raman shifts with pressure for second-order and first-order modes is presented in Fig. 2(b). We read each possible peak position instead of applying the multi-peak fitting for the second-order Raman cannot be described by damped harmonic oscillations. Apart from the soft mode A_{1g}, these mode frequencies increase linearly with pressure, and the slopes of the first-order modes are half of the minimal slopes measured for the second-order features. Combining our Raman analysis and inelastic x-ray results in previous results,[13] we can conclude that the anti-ferrodistortive cubic-tetragonal

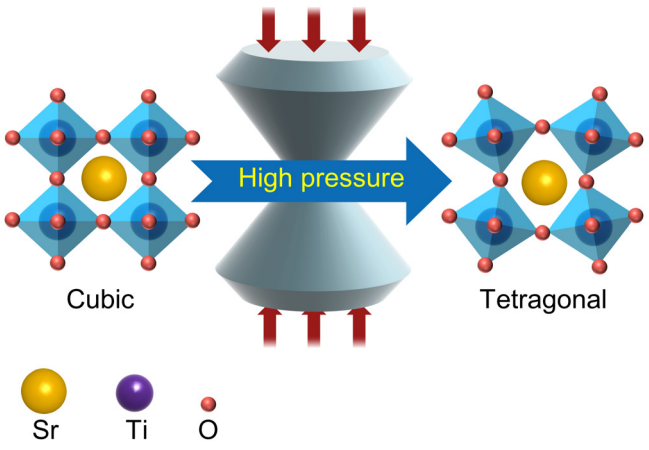

FIG. 1. The schematic diagram of the pressure-induced cubic rotation to tetragonal structure of $SrTiO_3$.

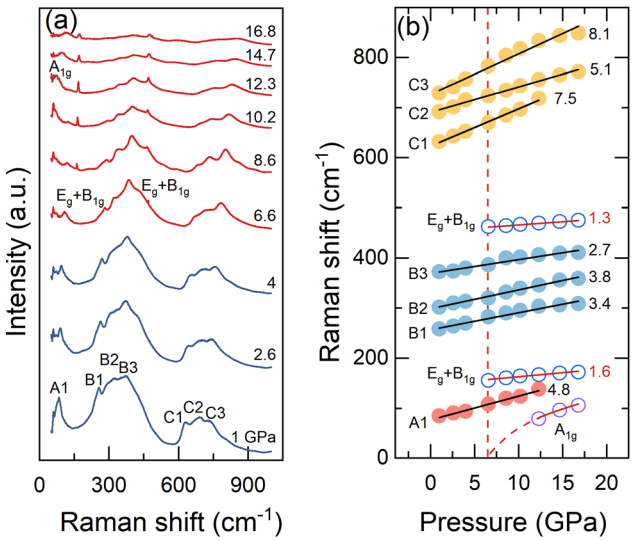

FIG. 2. (a) Selection of Raman spectra recorded with pressure. Peak positions of second-order modes are assigned using letters A, B, and C in an alphabetical order from low to high frequencies. $E_g + B_{1g}$ and A_{1g} are assigned as the first-order mode and the soft mode, respectively. (b) Evolution of the Raman shifts with pressure for second-order (solid symbols) and first-order modes from the tetragonal phase (open symbols). The slopes of these modes are from 1.3 to 8.1 cm^{-1}/GPa labeled in (b).

transition associates with the elongation and tilt of the TiO_6 octahedral in the tetragonal phase,[15] which leads to strongly nonlinear couplings among the structural order parameter, the volume strain, and the applied pressure. We also find that the width of second-order bands sharpens and the intensity weakens with compression. The behaviors of second-order features imply that Ti-O stretching and bending vibrations are becoming more harmonic with increased pressure, which indicates the atoms better ordered on their lattice sites accordingly.[22] Therefore, according to the analysis of Raman scattering results, it is obvious that investigating the phonon transport behaviors of $SrTiO_3$ can help reveal the effect of pressure-induced structural transitions, so that deepen our understanding of the structure–property relationships.

We subsequently conduct high-pressure TDTR experiments to investigate the κ of $SrTiO_3$ up to ~20 GPa. Analyzing TDTR signals requires adjusting unknown parameters to minimize the differences between the experimental data and theoretical model. Bidirectional heat flows into both $SrTiO_3$ and silicone-oil are considered.[24] Except for κ of $SrTiO_3$ and interfacial thermal conductance G of Al/$SrTiO_3$ extracted from the fitting, other parameters are determined carefully in the supplementary material, including κ of silicone-oil, volumetric heat capacity C of silicone-oil, Al, and $SrTiO_3$, and thickness h of Al (Fig. S2 in the supplementary material). We also confirmed that the accuracy on the κ measurement is highly sufficient through a sensitivity analysis of main parameters to the TDTR signal, shown in Fig. S4 of the supplementary material, where a high sensitivity can be found on the κ of $SrTiO_3$. Figure 3(a) illustrates the fitted ratio signals at the selected pressure. A wavy oscillation feature can be seen due to the Brillouin scattering of silicone-oil, which reflects that Al is not in contact with the anvil (Fig. S5 in the supplementary material).[25]

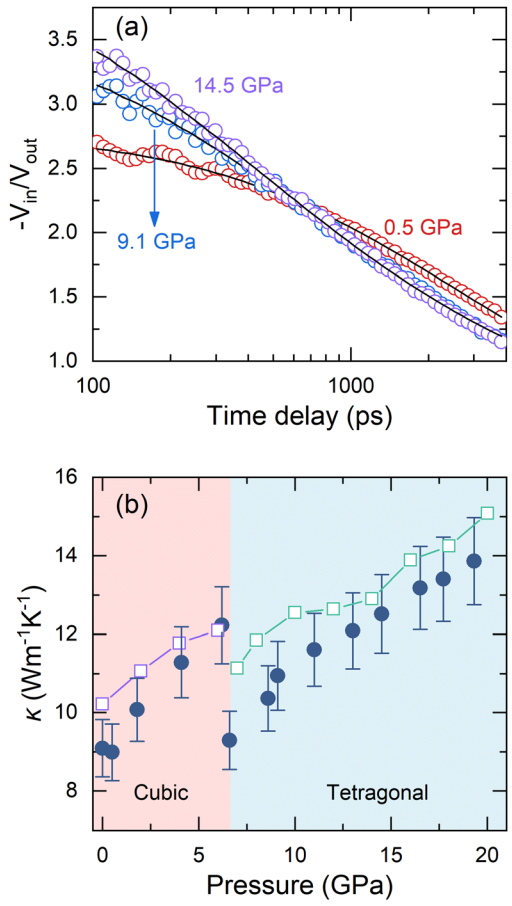

FIG. 3. (a) The ratio signal of in-phase (V_{in}) and out-of-phase (V_{out}) voltages fitted with the theoretical model at the selected pressure. (b) κ of $SrTiO_3$ as a function of pressure. Solid symbols are experimental results, and the open ones are from first-principles calculations.

The experimental pressure-dependent κ of $SrTiO_3$, which is summarized in Fig. 3(b) by solid circles, increases monotonously with compression in the cubic phase, and the increment is ~34%. While the anti-ferrodistortive cubic-tetragonal transition occurs at around 6 GPa, κ of $SrTiO_3$ drops from 12.2 to 9.3 W m^{-1} K^{-1} markedly. With the continued compression, the measured values rise again. The pressure-dependent κ of $SrTiO_3$ has similar trends with that of NaCl measured by Hsieh,[26] while the basic physical mechanism of this phenomena is different. The relevant analysis will be provided later. The pressure-dependent κ is calculated by first-principles calculations, and the details of which are described in the supplementary material. As shown in Fig. 3(b), the measured values nicely consist with our calculated results (open squares).

To reveal the underlying mechanism responsible for κ of $SrTiO_3$ behaviors, we conduct detailed analysis at the phonon mode level. In our calculations, three-phonon scattering instead of four-phonon scattering is considered for it can describe thermal behaviors of $SrTiO_3$ with adequate accuracy.[27] By solving the eigenvalues of the dynamical matrix extracted from the harmonic interatomic force constants, we obtain the phonon dispersion and phonon density of states (PDOS) of $SrTiO_3$ for the cubic phase at 0 GPa [Fig. 4(a)] and the tetragonal phase at 7 GPa [Fig. 4(b)]. We find that the dispersions of acoustic phonons are quickly flattened as the wavevector moves away from the zone center. Compared with acoustic branches, some of the optical branches are dispersive, which imply that their contributions to κ are not negligible. Prior studies[28,29] have demonstrated that the contribution of optical phonons to κ are important in nanostructured materials, and their effects on κ of bulk $SrTiO_3$ need to be further considered. To quantify the contribution of acoustic and optical phonons on κ of bulk $SrTiO_3$, we calculate the frequency distribution of κ of $SrTiO_3$ for the cubic phase at 0 GPa and the tetragonal phase at 7 GPa, shown in Fig. 4(c). We notice that the contribution to κ mainly originates from the phonons with 0–15 THz, especially above 5 THz, for both cubic and tetragonal phases. From the phonon dispersion and PDOS, the phonon frequency above 5 THz is optical branches. The coupling of acoustic and optical phonons arising from the strongly inharmonic mode limit the contribution of acoustic phonons to κ.[30] As a consequence, the contribution of acoustic phonons to the total κ is suppressed to less than 30% while the optical phonons, thus, contribute to more than 70%. Therefore, optical phonons seem to be the dominant heat carriers in $SrTiO_3$.

To elucidate the influence of pressure and phase-transition on κ behaviors, we analyze phonon properties. According to the classical kinetic theory, κ can be expressed as[31]

$$\kappa = \sum_{\lambda} C_{ph} (v_g)^2 \tau_{\lambda}, \quad (1)$$

where C_{ph} is the phonon heat capacity, v_g is the phonon group velocity, τ is the phonon relaxation time, and λ represents the wavevector and polarity of a phonon mode. Figure 4(d) depicts the average v_g within 15 THz as a function of pressure, and frequency dependent v_g at the selected pressure is shown in Fig. S6 of the supplementary material. We find that the average v_g increases monotonously with pressure in the cubic phase. When the cubic phase changes to the tetragonal phase, it drops markedly. In the tetragonal phase, however, the average v_g reduces with increasing pressure. Another phonon property governing κ is the τ. Figure 4(e) shows the frequency dependent τ at 0 and 20 GPa. It can be found that the τ of 0–15 THz increases with pressure. The quite high τ for 20 GPa at about 17 THz is rooted in the numerical instability of an iteration algorithm in ShengBTE package (see Fig. S7 in the supplementary material). Regarding to the C_{ph} which is shown in Fig. S2(a) in the supplementary material, it also slightly increases with pressure at cubic and tetragonal phases. Therefore, according to Eq. (1) and separate analyses of C_{ph}, v_g, and τ, it seems that all three components contribute positively to κ in the cubic phase, and κ plummets during phase transitions due to the reduction in v_g. In the tetragonal phase, C_{ph} and τ are still positive contributions to κ, whereas v_g is the opposite.

Since κ relates to the sum of the contribution from each phonon mode, we here try to separately adjust C_{ph}, v_g, and τ of each phonon mode in the κ calculations in order to discuss their effect on κ theoretically. As shown in Fig. 5(a), we replace each of the three components with high-pressure values, while the other two remain the initial value of each phase. For instance, when looking into the C_{ph} effect, κ was calculated using C_{ph} of high-pressure values while v_g and τ using either the constants at 0 GPa for cubic or the ones at 7 GPa for tetragonal

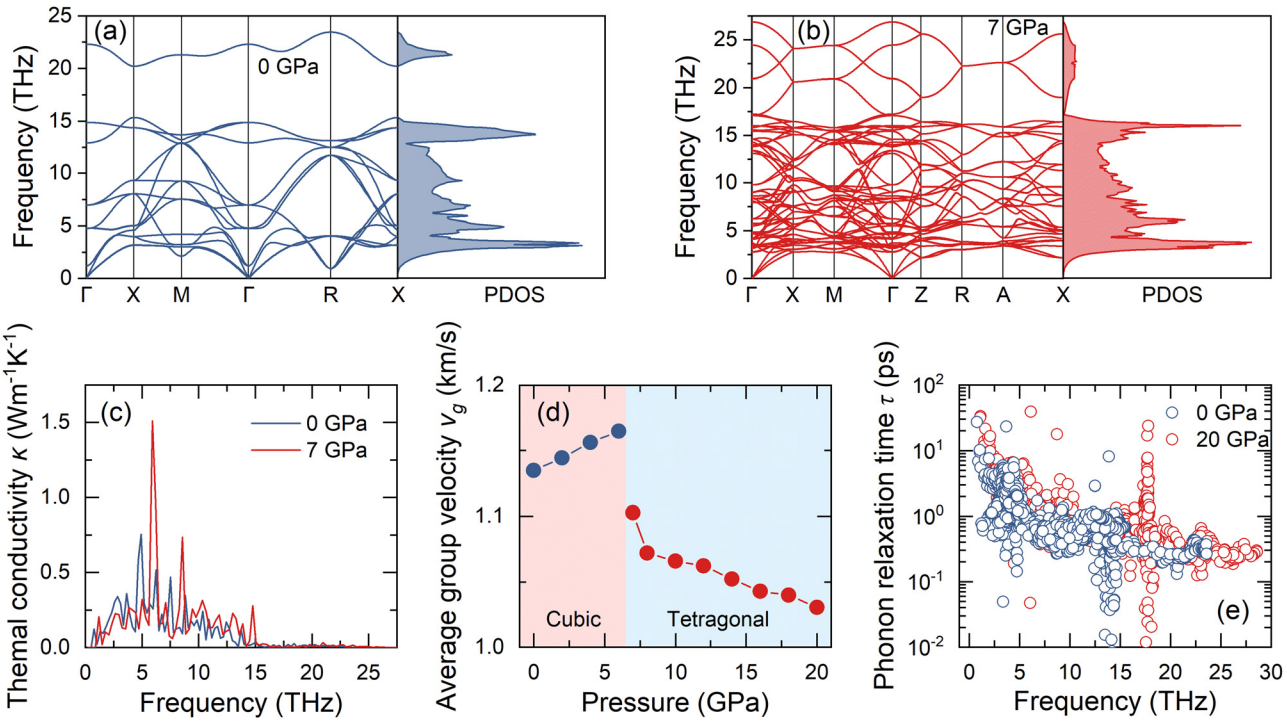

FIG. 4. Phonon dispersion curves and phonon density of states (PDOS) for (a) the cubic phase at 0 GPa and (b) the tetragonal phase at 7 GPa. (c) Frequency distribution of lattice thermal conductivity κ of $SrTiO_3$ at 0 and 7 GPa. (d) Average phonon group velocity v_g as a function of pressure. (e) Phonon relaxation time τ as a function of frequency at 0 and 20 GPa.

phases. Specifically, in the cubic phase, the replaced κ by pressure-dependent v_g and τ of each phonon mode increases with compression. However, the replaced κ by high-pressure C_{ph} of each phonon mode decreases slightly with compression despite the increase in total C_{ph}. Thus, the enhancement of κ by v_g and τ surpasses the reduction of κ by C_{ph}, making κ increases monotonously. According to the average v_g and the trend of the replaced κ by v_g and τ, we believe that the reduction of v_g governs the drop in κ after phase transitions. That is, the elongation and tilt of the TiO_6 octahedral induced by the soft-phonon-mode reduce the v_g. On the other hand, in the tetragonal phase, τ makes great positive contributions on κ while the replaced κ by C_{ph} and v_g decreases with increasing pressure, which means that τ is the dominant factor for κ of $SrTiO_3$. This observation supports our Raman scattering results that Ti-O stretching and bending vibrations are becoming more harmonic with compression.

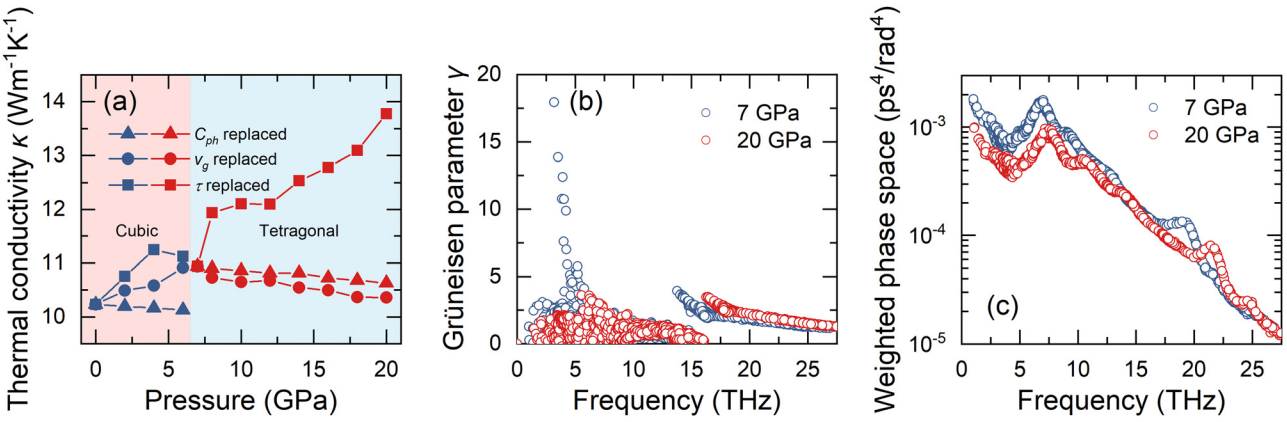

FIG. 5. (a) Calculated κ with C_{ph}, v_g, and τ of each phonon mode separately replaced by high-pressure values. (b) The frequency-dependent Grüneisen parameter γ of $SrTiO_3$ with the tetragonal phase at 7 and 20 GPa. (c) The frequency-dependent weighted phase space of $SrTiO_3$ with the tetragonal phase at 7 and 20 GPa.

格林乃森常数

Generally, Grüneisen parameter γ reflects the anharmonicity of phonon modes, as well as the weighted phase space characterizes the number of available phonon scattering channels. Hence, to further reveal the increase in τ of the tetragonal phase, we calculated the γ and the weighted phase space for three-phonon scattering. As shown in Fig. 5(b), within the major phonon frequency range that contributing to the thermal transport (0–15 THz), the γ at 7 GPa is larger than that of 20 GPa, indicating that pressure can benefit the harmonicity of phonon scattering.[32] For the weighted three-phonon scattering phase space of 7 and 20 GPa, as shown in Fig. 5(c), it can be seen that the phase space of 0–15 THz at 7 GPa is also larger than that of 20 GPa. As a result, more three-phonon scattering processes in lower pressure.[32] Therefore, we can conclude that in the tetragonal phase, the increase in τ is attributed to the decreasing in both γ and the weighted phase space, which reduce the anharmonicity of phonon modes and the phonon scattering channels, respectively.

In summary, the pressure dependent κ of $SrTiO_3$ was experimentally and theoretically investigated up to ~20 GPa. Our first principles calculations well explain the measured κ by the TDTR technique. We find that optical phonons dominate κ of $SrTiO_3$ in both cubic and tetragonal phases. On the contrary, in the pressure range of the cubic phase, the increase in v_g and τ makes κ increase monotonously with compression. During the transitions from the cubic to tetragonal phase, the significant drop in κ is dominated by the reduced v_g, which originally results from the elongation and tilt of the TiO_6 octahedral induced by the soft-phonon-mode. In the tetragonal phase, the monotonically increased κ with compression mainly relies on the reduction of the anharmonicity of phonon modes and the phonon scattering channels. Our results not only help reveal the pressure effect on κ of complex oxides but also pave their way for applications on high-temperature superconductors and spin devices.

See the supplementary material for more details on sample preparations, TDTR experiments, high-pressure Raman spectroscopy, first-principles calculations, and some supporting data.

The authors are supported by the National Natural Science Foundation of China (Grant Nos. 51720105007 and 51976025) and the Fundamental Research Funds for the Central Universities [Grant No. DUT20RC(5)023].

AUTHOR DECLARATIONS

Conflict of Interest

The authors have no conflicts to disclose.

Author Contributions

Zhongyin Zhang: Investigation (lead); Methodology (equal); Writing – original draft (lead); Writing – review and editing (equal). **Kunpeng Yuan:** Investigation (equal); Methodology (equal); Writing – review and editing (equal). **Jie Zhu:** Conceptualization (equal); Funding acquisition (equal); Supervision (equal); Writing – review and editing (equal). **Xuanhui Fan:** Investigation (equal); Methodology (equal). **Jing Zhou:** Investigation (supporting); Methodology (supporting); Writing – review and editing (supporting). **Dawei Tang:** Conceptualization (equal); Funding acquisition (lead); Supervision (lead); Writing – review and editing (equal).

DATA AVAILABILITY

The data that support the findings of this study are available from the corresponding authors upon reasonable request.

REFERENCES

[1]S. Sadhu, T. Buffeteau, S. Sandrez, L. Hirsch, and D. M. Bassani, J. Am. Chem. Soc. **142**, 10431 (2020).
[2]N. Phung, R. Félix, D. Meggiolaro, A. Al-Ashouri, G. Sousa e Silva, C. Hartmann, J. Hidalgo, H. Köbler, E. Mosconi, B. Lai, R. Gunder, M. Li, K.-L. Wang, Z.-K. Wang, K. Nie, E. Handick, R. G. Wilks, J. A. Marquez, B. Rech, T. Unold, J.-P. Correa-Baena, S. Albrecht, F. De Angelis, M. Bär, and A. Abate, J. Am. Chem. Soc. **142**, 2364 (2020).
[3]Q. Li, Y. Wang, W. Pan, W. Yang, B. Zou, J. Tang, and Z. Quan, Angew. Chem. Int. Ed. **56**, 15969 (2017).
[4]T. F. Nova, A. S. Disa, M. Fechner, and A. Cavalleri, Science **364**, 1075 (2019).
[5]S. Latini, D. Shin, A. Sato Shunsuke, C. Schäfer, U. De Giovannini, H. Hübener, and A. Rubio, Proc. Natl. Acad. Sci. **118**, e2105618118 (2021).
[6]G. A. Samara, T. Sakudo, and K. Yoshimitsu, Phys. Rev. Lett. **35**, 1767 (1975).
[7]K. Ahadi, L. Galletti, Y. Li, S. Salmani-Rezaie, W. Wu, and S. Stemmer, Sci. Adv. **5**, eaaw0120 (2019).
[8]H. Yang, F. Yan, Y. Lin, and T. Wang, Appl. Phys. Lett. **111**, 253903 (2017).
[9]A. F. Santander-Syro, F. Fortuna, C. Bareille, T. C. Rödel, G. Landolt, N. C. Plumb, J. H. Dil, and M. Radović, Nat. Mater. **13**, 1085 (2014).
[10]T. Ishidate, S. Sasaki, and K. Inoue, High Pressure Res. **1**, 53 (1988).
[11]M. Guennou, P. Bouvier, J. Kreisel, and D. Machon, Phys. Rev. B **81**, 054115 (2010).
[12]A. Kiraci and H. Yurtseven, J. Am. Ceram. Soc. **101**, 1344 (2018).
[13]S.-C. Weng, R. Xu, A. H. Said, B. M. Leu, Y. Ding, H. Hong, X. Fang, M. Y. Chou, A. Bosak, P. Abbamonte, S. L. Cooper, E. Fradkin, S. L. Chang, and T. C. Chiang, Europhys. Lett. **107**, 36006 (2014).
[14]P. A. Fleury, J. F. Scott, and J. M. Worlock, Phys. Rev. Lett. **21**, 16 (1968).
[15]E. K. H. Salje, M. Guennou, P. Bouvier, M. A. Carpenter, and J. Kreisel, J. Phys.: Condens. Matter **23**, 275901 (2011).
[16]H. Zhang, S. Liu, M. E. Scofield, S. S. Wong, X. Hong, V. B. Prakapenka, E. Greenberg, and T. A. Tyson, Appl. Phys. Lett. **111**, 052904 (2017).
[17]A. Hachemi, H. Hachemi, A. Ferhat-Hamida, and L. Louail, Phys. Scr. **82**, 025602 (2010).
[18]L. Khaber, A. Beniaiche, and A. Hachemi, Solid State Commun. **189**, 32 (2014).
[19]Z. Zhang, Z. Chang, X. Fan, J. Zhou, X. Wang, G. Li, X. Zhang, J. Zhu, and D. Tang, iScience **24**, 102990 (2021).
[20]X. Meng, T. Pandey, J. Jeong, S. Fu, J. Yang, K. Chen, A. Singh, F. He, X. Xu, J. Zhou, W.-P. Hsieh, A. K. Singh, J.-F. Lin, and Y. Wang, Phys. Rev. Lett. **122**, 155901 (2019).
[21]G. T. Hohensee, R. B. Wilson, and D. G. Cahill, Nat. Commun. **6**, 6578 (2015).
[22]A. Grzechnik, G. H. Wolf, and P. F. McMillan, J. Raman Spectrosc. **28**, 885 (1997).
[23]T. Ishidate and T. Isonuma, Ferroelectrics **137**, 45 (1992).
[24]A. Schmidt, M. Chiesa, X. Chen, and G. Chen, Rev. Sci. Instrum. **79**, 064902 (2008).
[25]Z. Zhang, X. Fan, J. Zhu, J. Zhou, and D. Tang, Rev. Sci. Instrum. **93**, 043904 (2022).
[26]W.-P. Hsieh, Sci. Rep. **11**, 21321 (2021).
[27]Q. Wang, Z. Zeng, and Y. Chen, Phys. Rev. B **104**, 235205 (2021).
[28]Z. Tian, K. Esfarjani, J. Shiomi, A. S. Henry, and G. Chen, Appl. Phys. Lett. **99**, 053122 (2011).
[29]S. Wang, X. Lu, A. Negi, J. He, K. Kim, H. Shao, P. Jiang, J. Liu, and Q. Hao, Eng. Sci. **17**, 45 (2022).
[30]L. Feng, T. Shiga, and J. Shiomi, Appl. Phys. Express **8**, 071501 (2015).
[31]G. Chen, Nat. Rev. Phys. **3**, 555 (2021).
[32]K. Yuan, X. Zhang, D. Tang, and M. Hu, Phys. Rev. B **98**, 144303 (2018).